I&EC research
Industrial & Engineering Chemistry Research
pubs.acs.org/IECR
Article

Predicting the Mixing Time of Soft Elastic Reactors: Physical Models and Empirical Correlations

Guillaume Delaplace,* Minghui Liu, Romain Jeantet, Jie Xiao,* and Xiao Dong Chen

Cite This: *Ind. Eng. Chem. Res.* 2020, 59, 6258−6268

ABSTRACT: The aim of this study was to experimentally determine the mixing times of viscous fluids placed in a soft container where they were mixed by the vibrations of the tank wall. In parallel, mechanistic models were established to link the inlet parameters of the crank/slider device responsible for the tank wall vibrations to the mixing times. The mechanistic models are based on dimensional analysis. Either momentum change (change in instantaneous velocity with which the slider comes in contact with the soft elastic reactor) or impulse (force transmitted by the piston) is introduced as an intermediate parameter in the relevant list of physical quantities in order to take the intensity of mechanical solicitation induced by the beater into account. These two intermediate parameters were theoretically computed on the basis of knowledge about the geometrical parameters and the rotational speed of the crank/slider device. The experimental results showed that the mixing time strongly depends on momentum change (or impulse) induced by the beater and its striking frequency. Empirical correlations are proposed, and good agreements between experimental and predicted values were obtained as the standard deviation is lower than 20% for the whole data set.

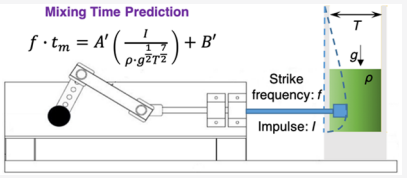

1. INTRODUCTION

Chen,[1] working on bioinspired chemical engineering reactors (BioChE defined by Chen, 2016), recently introduced a new homogenization system referred to as a soft elastic reactor (SER) to the mixing community.[2−6]

This mixing system consists of a soft container that can achieve homogenization through vibrations of the tank wall (Figure 1). With no agitator in contact with the agitated media, it offers advantages for many potential mixing applications, both at the laboratory and at the industrial scale, as previously reported by Delaplace et al. (2018).[7] Two relevant applications of this mixing equipment in the field of chemical engineering are (i) disposable containers, facilitating sterilization and skipping cleaning steps compared to traditional bioreactors used for microbial cultivation, and (ii) mixing operations involving highly corrosive media as any problem of corrosion of the agitator is eliminated in this case.

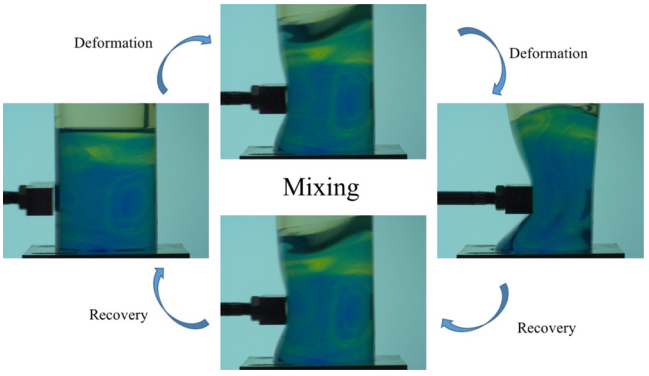

Figure 1. Mixing process of an SER showing cyclic deformation and recovery of the reactor wall. The tip of the piston of a slider crank device is shown here.

It should be noted that fluid homogenization induced by fluctuating external perturbations has attracted little attention until now in the mixing community. The current lack of experimental data on the parameters governing the homogenization course in such mixing equipment as well as the absence of predictive models describing the performance of such mixing systems are obstacles to be overcome to convince engineers to use this mixing system more extensively.

An interesting contribution was recently made in this field by Delaplace et al. (2018) using the dimensional analysis approach.[7] Specifically, three groups of dimensionless numbers were found to influence the mixing progress. In particular, these dimensionless numbers include (i) those containing the variables responsible for wall vibrations (i.e., the maximum penetration depth, the height of the beater from the bottom of the tank, and the angular frequency of the beater); (ii) dimensionless numbers characterizing the deformation and recovery of the soft elastic wall (i.e., the elastic properties of the material, wall thickness, and clamp protocol); and (iii)

Received: November 6, 2019
Revised: February 29, 2020
Accepted: March 5, 2020
Published: March 5, 2020

https://dx.doi.org/10.1021/acs.iecr.9b06053
Ind. Eng. Chem. Res. 2020, 59, 6258−6268

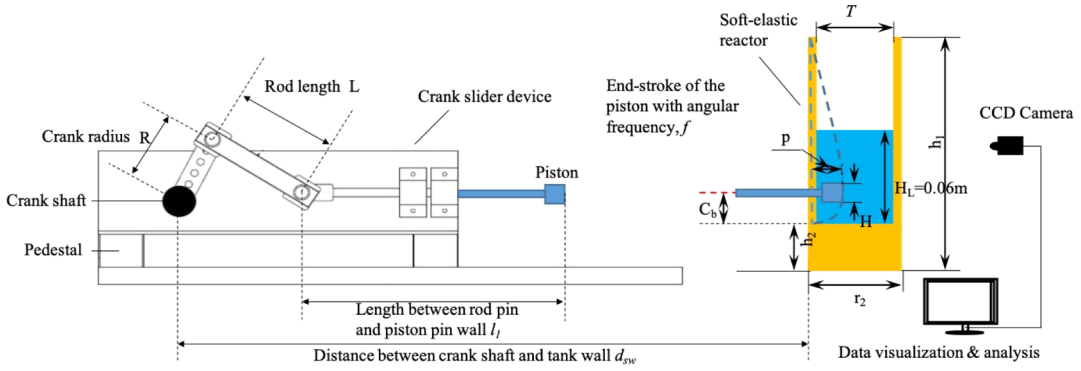

Figure 2. Sketch and geometrical parameters of the drive system (crank/slider device, left side) of the SER and of the digital image acquisition system (right).

dimensionless ratios defining the liquid properties contained in the tank and the liquid height.

This modeling effort has allowed us to define two dimensionless numbers: the mixing time (θ_m) and the Reynolds (Re) number for this special type of mixing equipment

$$\theta_m = f \cdot t_m \tag{1}$$

$$Re = \frac{\rho \cdot f \cdot T^2}{\mu} \tag{2}$$

In eqs 1 and 2, t_m is the mixing time required to obtain the desired degree of homogeneity, whereas ρ and μ are the density and viscosity, respectively, of the agitated Newtonian media to be homogenized. f, refers to the striking frequency of the beater, while T is the container diameter.

More precisely, for a given tank containing a fixed liquid height and a given position of beater strikes on the outside wall of the reactor, Delaplace et al. (2018) reported that the mixing time number depends on four dimensionless numbers[7]

$$\theta_m = F_1\left(Re,\ Ga,\ \frac{p}{T},\ \frac{C_b}{T}\right) \tag{3}$$

where $Ga = \frac{g \cdot T^3 \rho^2}{\mu^2}$ is the Galilei number of the SER, whereas p/T and C_b/T are two geometrical ratios that describe the beater action and position. In eq 3, the Galilei number is an internal measurement (consisting of repeated physical quantities specific to the studied mixing system) that takes the effect of gravity on the free surface of the liquid into account. The Galilei impact is supposed to be significant when free surface of the liquid is no longer flat and vortex is capable of changing the mixing progress. p/T is a ratio arising from the fact that different maximum penetration depths, p, could be set. Note that the maximum penetration depth p with which the beater periodically deforms the soft elastic wall was measured by Delaplace et al. (2018).[7] However, this value could also be deduced from the knowledge of the geometrical parameters of the crank/slider device (including the crank radius R, the rod length L, and the distance from the rod pin to the piston pin l_1) and of the distance separating the crankshaft center to the vertical tank wall (d_{sw}), as shown in Figure 2.

$$p = d_{sw} - R - L - l_1 \tag{4}$$

C_b/T is a ratio that takes the bottom clearance of the beater into account. Note that various distances between the horizontal axis that defines the beater course C_b and the tank bottom could be used for our setup.

Delaplace et al. (2018)[7] also carried out experimental measurements of mixing times by varying parameters p, C_b, f, and the viscosity of Newtonian fluids. Their study provides insights into the shape of the mixing curve and influential parameters.

Based on the capabilities of the experimental system, the range of varying parameters was chosen to cover the largest flow range regimes in the container, that is, from the laminar regime ($Re < 3$) to the turbulent mixing regime ($Re > 60$). The main information collected from experimental data could be briefly summarized as follows:

- For the experimental range investigated, analysis of mixing time data shows that the SER mixing number mainly depends on Reynolds numbers, is slightly affected by (C_b/T), and not influenced by the Galilei number value. The absence of free surface deformation was clearly noted by the authors for the operating conditions applied in this work, and it is therefore expected that the Galilei number should be negligible for these experiments. Moreover, the authors suggest that the impact of (C_b/T) on mixing time was expected to be weak because the ratio between the tank diameter and the liquid height T/H_L is equal to 0.833, and, in this context, it could be assumed that wall deformation is strong enough to induce convection motion in the whole tank. This will not necessarily be the case if this ratio becomes higher.
- Analysis of the form of the mixing curve for a given maximum penetration depth ratio (equal to a p/T of 0.42) revealed that, under a laminar regime, a fixed number of strikes, $f \cdot t_m$, is necessary to obtain the targeted homogeneity level. On the contrary, a drastic decrease in the number of strikes is reported when the transition regime is reached.

It can be observed that the number of strikes required to achieve the desired homogeneity level increases when p/T decreases, but the sigmoidal shape of the mixing curve remains similar, regardless of the fixed p/T values. However, this increasing number of strikes required to reduce heterogeneity with decreasing p/T values also seems to be significantly influenced by the flow regime (Reynolds number). This trend is not illogical from a physical point of view because the convection of liquid elements induced by the deformation of the soft elastic surface is supposed to have a greater influence

https://dx.doi.org/10.1021/acs.iecr.9b06053
Ind. Eng. Chem. Res. 2020, 59, 6258−6268

when the flow regime is laminar in comparison to transition and turbulent regime, the molecular diffusion being restricted in this case.

Finally, the authors emphasized that the S-shaped mixing curves of the SER are very similar to those obtained with traditional mixers such as helical ribbon agitators used for homogenizing liquids. They mentioned that some analogies exist between the mixing curves of classical mixing systems (for which an agitator performs one revolution around a vertically centered axis) and this SER. For a tank equipped with one central agitator, a fixed number of revolutions of the agitator should be completed in order to obtain the targeted homogeneity level. Here, for the SER, a fixed number of strikes are necessary for obtaining the desired degree of homogeneity. In the two cases, the displacement of a tool (an agitator inside the tank or a beater outside the container) is responsible for the mixing progress.

The pioneering study of Delaplace et al. (2018) is the only one that includes a dimensional analysis on an SER, paving the way for the identification of the key dimensionless numbers that govern homogenization operations.[7] This approach also gave a first idea about controlling the mixing dynamics of liquids in an SER and allowed a comparison with homogenization mechanisms achieved by classical mixers.

Unfortunately, this preliminary "blind dimensional analysis" was not fully satisfactory. This approach can only provide limited insights into the physics governing the mixing time of the SER. Physical quantities such as impulse induced by the piston or change in momentum of the piston induced by the strike, which are considered to be the underlying parameters of the mixing process, did not appear in the model. Consequently, at this stage, it is difficult to determine how the maximum penetration depth of the beater and the angular frequency of the crank contribute to modifying the impulse or change in momentum provided by the beater. Moreover, no empirical process relationship was proposed to correlate the mixing time with the operating parameters (i.e., causal inlet variables).

To fill this gap, it was decided

(i) to make a dimensional analysis for a second time, introducing an intermediate variable with full physical meaning into the relevant list, that is, impulse or change in momentum induced by the strike. This is not an easy task because analytical estimation of these intermediate physical quantities required analysis of the kinetic motion of the piston. Precisely, an expression of these physical quantities and their variations based on the knowledge of the inlet parameters of the crank mechanism [the angular frequency of the crank (in cycles/second) and the distance separating the crankshaft center to the vertical tank wall (in meters)] should be theoretically established.

(ii) to reanalyze the experimental data in this new π-space in order to propose predictive empirical correlations of mixing time that involve change in momentum or impulse.

2. MATERIALS AND METHODS

2.1. SER under Investigation. Figure 1 shows the deformation and the recovery of the container wall upon the beater strike. Figure 2 illustrates the three main parts constituting the SER: a transparent container with elastic walls, a slider crank device to deform periodically the wall by a piston tip, and a camera that allows us to obtain digital images of mixing progress.

Figure 2 reports the geometrical parameters that are required to describe the container and the position of the beater. The total height, h_1, the external diameter, r_2, and the base height at the bottom, h_2, of the soft elastic tank were 0.15, 0.06, and 0.03 m, respectively. The height of the liquid inside the tank H_L was 0.06 m. The internal diameter of the tank T was 0.05 m. The bottom part of the container was "clamped" to ensure a good fixature. The geometrical parameters of the crank/slider device are also included in Figure 2. The crank radius R, the rod length L, and the distance from the rod pin to the piston pin l_1 were 0.035, 0.14, and 0.21 m, respectively. Note that the crank/slider device induces a displacement of the piston pin along the horizontal axis. In fact, the piston oscillates around the soft container wall. Depending on the angle between the crank and the horizontal axis, the abscissa of the piston on the horizontal axis varies. Consequently, for a fixed crank/slider device and a given distance between the crankshaft and the vertical wall of the container (d_{sw}), the maximum penetration depth p varies.

2.2. Mixing Fluid. The liquids to be homogenized are Newtonian media with a viscosity (μ) varying from 0.0285 to 1.187 Pa·s. Their density (ρ) was measured in between 1190 and 1272 kg/m^3. These two liquid properties were considered at 25 °C, which corresponds to the bulk temperature of the fluid inside the tank.

2.3. Mixing Time Measurements. The mixing time was deduced by analyzing the color change in the fluid induced by a decolorization reaction. The injected acidic fluid has properties similar to the agitated basic media. The reliability and repeatability of the colorimetric diagnosis applied to an SER has recently been achieved.[5] The mixing time was defined as the duration from the injection up to the time instant for which the degree of homogeneity becomes consistently higher than 90%. All details concerning the injection of the acidic liquid into the basic agitated media, decolorization monitoring, the definition of the degree of homogeneity, and the determination of mixing time are the same as those given in previous publications by Delaplace et al. (2018) and will not be repeated here for the sake of brevity.[7] During mixing experiments, the maximum penetration depth $p = d_{sw} - R - L - l_1$, the bottom clearance, C_b, and the crank slider frequency, f, have been set from 0.015 to 0.025, 0.025 m, and 0.5−3.0 cycles/s, respectively.

2.4. Impulse Evaluation. As shown in eq 5, the impulse is the integration of the transversal force of the piston (which corresponds to the x-component force exerted by the piston pin), $F_p(\theta)$ (Figure 3), within the interval of time defined between the instant t_c when the piston comes in contact with the soft container ($\theta = \theta_c$) and the instant t_p at which the maximum penetration depth of the piston in the soft reactor ($\theta = \theta_p$) occurs.

$$I = \int_{t_c}^{t_p} F_p(\theta)\, dt \tag{5}$$

Consequently, evaluation of the impulse requires the analytical expression of $F_p(\theta)$ and the knowledge of the two instants of time, t_c and t_p. The well-known rectangular method was used to approximate the definite integral that appears in eq 5.

The following assumptions were made: (i) the weights of the crank and the follower can be neglected; (ii) the slider

https://dx.doi.org/10.1021/acs.iecr.9b06053
Ind. Eng. Chem. Res. 2020, 59, 6258−6268

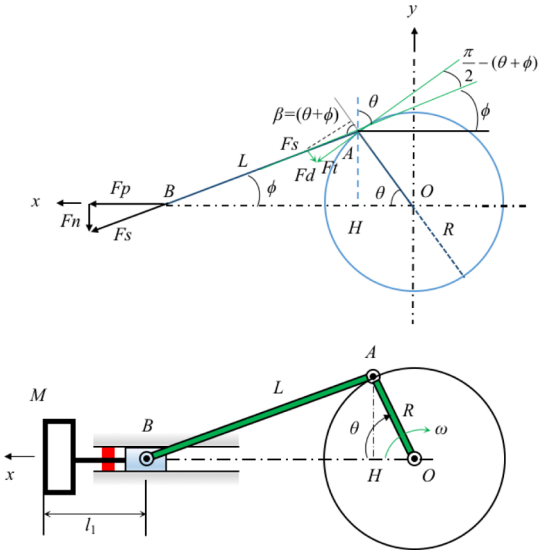

Figure 3. Kinetic motion of a crank/slider device and forces induced by the crank mechanism.

crank mechanism is a totally frictionless system; and (iii) the crank rotates clockwise at a constant angular velocity, $\dot{\theta} = \omega$ (Figure 3), and the x-component force exerted by the slider F_p can be theoretically obtained from the knowledge of the instantaneous acceleration of the piston, $\text{acc}(\theta) = \left\| \frac{d^2\overrightarrow{OB}}{dt^2} \right\|$

$$F_p(\theta) = m_{\text{piston}} \cdot \left\| \frac{d^2\overrightarrow{OB}}{dt^2} \right\| \tag{6}$$

In eq 6, m_{piston} is the piston mass (i.e., 0.06093 kg in this study). Note that in eq 6, the piston mass is sometimes replaced by a reciprocating mass, which corresponds to the piston mass, plus approximately two-third of the connecting rod mass. In this case, the piston mass was used.

It can be shown that the instantaneous acceleration, $\left\| \frac{d^2\overrightarrow{OB}}{dt^2} \right\| = \left\| \frac{d^2\overrightarrow{OM}}{dt^2} \right\|$, can be deduced by differentiating the displacement of the piston $\overrightarrow{OM}$ with respect to the crank angle θ, which can be derived using simple trigonometry.

Indeed, from Figure 3, it can be observed that

$$\overrightarrow{OM} = \overrightarrow{OA} + \overrightarrow{AB} + \overrightarrow{BM} \tag{7}$$

which becomes

$$\overline{OM} = R\cos\theta + L\cos\varnothing + l_1 \tag{8}$$

On the basis of Figure 3, it can be also established that

$$\text{HA} = \sin\varnothing \cdot L = R\cdot\sin\theta \tag{9}$$

Consequently

$$\varnothing = \arcsin\left[\frac{R}{L}\cdot\sin\theta\right] \tag{10}$$

and

$$\cos\varnothing = \cos\left(\arcsin\left[\frac{R}{L}\cdot\sin\theta\right]\right) = \left(1 - \left[\frac{R}{L}\cdot\sin\theta\right]^2\right)^{1/2} \tag{11}$$

Introducing eq 11 into 8 gives 12

$$\overline{OM} = R\cos\theta + L\left(1 - \left[\frac{R}{L}\cdot\sin\theta\right]^2\right)^{1/2} + l_1 \tag{12}$$

Taking the derivative of eq 12 with respect to time gives

$$V(\theta) = \left\| \frac{d\overrightarrow{OM}}{dt} \right\| = -R\cdot\sin\theta\cdot\omega - L\cdot\left(1 - \left[\frac{R}{L}\cdot\sin\theta\right]^2\right)^{-1/2}\left[\frac{R}{L}\right]\cdot\sin\theta\cdot\omega\cdot\cos\theta\cdot\left[\frac{R}{L}\right] \tag{13}$$

where

$$\dot{\theta} = \omega = 2\cdot\pi\cdot f \tag{14}$$

The derivative of eq 10 gives

$$\frac{d\varnothing}{dt} = \left(1 - \left[\frac{R}{L}\cdot\sin\theta\right]^2\right)^{-1/2}\cdot\omega\cdot\cos\theta\cdot\left[\frac{R}{L}\right] = \omega\cdot\frac{R}{L}\cdot\left[\frac{\cos\theta}{\cos\varnothing}\right] \tag{15}$$

Combining eq 15 with 13 also gives

$$V(\theta) = \left\| \frac{d\overrightarrow{OM}}{dt} \right\| = \left\| \frac{d\overrightarrow{OB}}{dt} \right\| = -R\cdot\sin\theta\cdot\left(\omega + \frac{d\varnothing}{dt}\right) \tag{16}$$

The derivative of eq 16 allows us to obtain the expression of piston acceleration (eq 17). It can be shown that

$$\left\| \frac{d^2\overrightarrow{OM}}{dt^2} \right\| = \left\| \frac{d^2\overrightarrow{OB}}{dt^2} \right\| = \text{acc}(\theta) = -R\cdot\omega\cdot\cos\theta\cdot\left(\omega + \frac{d\varnothing}{dt}\right) - R\cdot\sin\theta\cdot\left(\left(\frac{d^2\varnothing}{dt^2}\right)\right) \tag{17}$$

where

$$\frac{d^2\varnothing}{dt^2} = \frac{(-R\cdot\omega^2\cdot[\sin\theta]) + L\cdot\left(\frac{d\varnothing}{dt}\right)^2\cdot\sin\theta}{L\cdot\cos\varnothing} \tag{18}$$

is obtained by taking the derivative of eq 15.

2.5. Change in Momentum Evaluation. Momentum is the product of piston mass multiplied by its velocity. The change in momentum (denoted as $m_{\text{piston}}\Delta V$) is the difference between the momentums evaluated at the instant t_c at which the piston comes in contact with the soft container and at the instant of time t_p at which the maximum penetration depth of the piston in the soft reactor occurs. For this last instant of time, the velocity of the piston becomes equal to zero. Consequently, the change in momentum can be rewritten as:

$$m_{\text{piston}}\Delta V = m_{\text{piston}}\cdot V(\theta = \theta_c) \tag{19}$$

In eq 19, $V(\theta = \theta_c)$ is the velocity of the piston evaluated at the angular position θ_c at which the piston comes in contact with the tank. The angular position θ_c at which the piston comes in contact with the tank depends on the fixed value of the maximum penetration depth p.

https://dx.doi.org/10.1021/acs.iecr.9b06053
Ind. Eng. Chem. Res. 2020, 59, 6258−6268

2.5.1. Evaluation of the Angular Position θ_c at Which the Piston Comes in Contact with the Tank. The piston comes in contact with the tank when

$$\overline{OM} = R + L + l_1 - p \tag{20}$$

Therefore, introducing eq 20 into 12, the crank angle θ_c at which the piston comes in contact with the tank could be obtained by rearranging eq 21

$$R + L + l_1 - p = R\cos\theta_c + L\left(1 - \left[\frac{R}{L}\cdot\sin\theta_c\right]^2\right)^{1/2} + l_1 \tag{21}$$

2.5.2. Evaluation of the Instant of Time t_c at Which the Piston Comes in Contact with the Tank. Consequently, the instant of time t_c at which the piston comes in contact with the tank could also be determined

$$t_c = \theta_c/\omega = \theta_c/(2\cdot\pi\cdot f) \tag{22}$$

2.5.3. Evaluation of the Velocity at Which the Piston Comes in Contact with the Tank ($\theta = \theta_c$). Knowledge of the crank angle θ_c at which the piston comes in contact with the tank allows us to evaluate the velocity of the piston when it is in contact with the soft reactor

$$V(\theta = \theta_c) = -R\cdot\sin\theta\cdot\omega - L\cdot\left(1 - \left[\frac{R}{L}\cdot\sin\theta_c\right]^2\right)^{-1/2}\left[\frac{R}{L}\right]\cdot\sin\theta_c\cdot\omega\cdot\cos\theta_c\cdot\left[\frac{R}{L}\right] \tag{23}$$

2.5.4. Evaluation of Angular Position θ_p at Which the Piston Reaches the Maximum Penetration Depth. The piston reached the maximum penetration depth when

$$\overline{OM} = R + L + l_1 \tag{24}$$

On the basis of Figure 3, it could be observed that this piston tip position is achieved when

$$\theta_p = 2\pi \tag{25}$$

For this angular position, the piston velocity, $V(\theta = \theta_p)$, becomes zero.

Consequently, the instant of time t_p at which the piston reaches the maximum penetration depth could also be determined

$$t_p = \theta_p/\omega = \theta_p/(2\cdot\pi\cdot f) = 1/f \tag{26}$$

3. RESULTS AND DISCUSSION

3.1. Dimensional Analysis of Mixing Time in SER with Impulse or Change in Momentum Introduced as Intermediate Variables. Dimensional analysis is a powerful tool to investigate the link that exists between the inlet and outlet parameters of a system and to determine the mathematical correlations that describe the causal relationship. In a recent book, Delaplace et al. (2015) reviewed in detail how dimensionless numbers should be rigorously constructed.[8] The recommended guidelines for applying a dimensional analysis were strictly implemented here, taking the mixing time measured in the container as the output and the operating parameters of the crank/slider device as the inlet of the studied system.

Figure 2 represents the soft elastic container hit by the beater of the crank slider device. Analysis of Figure 2 clearly shows that the liquid homogenization in such a reactor is influenced by the following variables:

- Geometrical parameters delimitating the flow domain. They include the container inner diameter, T, and the liquid height, H_L. Because a field of gravity exists at the free surface of the liquid, acceleration g should not be omitted, although it is a constant in all experiments.
- Material properties of the fluids in the SER. These agitated liquids are Newtonian fluids. Consequently, density (ρ) and viscosity (μ) are intrinsic properties and constant in all the volume of the vessel. Note that the diffusion coefficient was not retained in the relevant list of parameters because it has been numerously and previously established that convection is preponderant for driving the mass transfer of such a system.
- Process parameters, namely:
  (1) The impulse I or the change in momentum $m_{piston}\Delta V$, which are the underlying physical quantities that have a significant influence on the mixing of fluids inside the vessel;
  (2) The period ($1/f$) of the collision between the beater and the container wall. f is the angular frequency of the crank (in rps).
- Parameters that describe the way the impulse or change in momentum is dissipated to the wall of the container and the definition of the recovery properties of the SER after deformation. Among them, we can include:
  (1) The height and width of the beater (in m), H and w, respectively, which define the contact surface with which the beater transmits the impulsion or change in momentum;
  (2) The bottom clearance of the piston C_b (i.e., the distance between the horizontal axis defining the beater course and the bottom of the tank) that defines the position at which the initial deformation is induced.

At the end of the of the maximum penetration depth, it is mandatory for the piston to retreat. Consequently, the deformed wall of the SER starts to recover (see Figure 1). This step is driven by the elastic properties and thickness of the vertical wall and is expected to influence the mixing course inside the container. Hence, it is important to integrate in the relevant list of the dimensional analysis the physical quantities responsible for this recovery behavior. In our work, the elastic modulus (also known as Young's modulus E) of the container material and some geometrical parameters that can characterize the SER behavior during recovery (e.g., height h_1, base height h_2, and outer diameter r_2 of the tank) have been listed.

Finally, depending on whether the impulse I or the change in momentum $m_{piston}\Delta V$ is introduced into the relevant list, the SER homogenizing process can therefore be expressed by the relationship

$$t_m = F_2(h_1, h_2, r_2, E, T, H_L, C_b, H, w, I, \rho, \mu, 1/f, g) \tag{27}$$

$$t_m = F_3(h_1, h_2, r_2, E, T, H_L, C_b, H, w, m_{piston}\Delta V, \rho, \mu, 1/f, g) \tag{28}$$

https://dx.doi.org/10.1021/acs.iecr.9b06053
Ind. Eng. Chem. Res. 2020, 59, 6258−6268

Choosing (T,ρ,g) as the repeated physical variables, the corresponding dimensionless ratios associated with SER mixing time are

$$\frac{t_m \cdot g^{1/2}}{T^{1/2}} = F_4\left(\frac{h_1}{T}, \frac{h_2}{T}, \frac{r_2}{T}, \frac{E}{\rho \cdot Tg}, \frac{H_L}{T}, \frac{C_b}{T}, \frac{H}{T}, \frac{w}{T}, \frac{I}{\rho \cdot g^{1/2} T^{7/2}}, \left(\frac{g \cdot T^3 \rho^2}{\mu^2}\right), \pi_1 = \left(\frac{g^{1/2}}{T^{1/2} \cdot f}\right)\right) \quad (29)$$

$$\frac{t_m \cdot g^{1/2}}{T^{1/2}} = F_5\left(\frac{h_1}{T}, \frac{h_2}{T}, \frac{r_2}{T}, \frac{E}{\rho \cdot Tg}, \frac{H_L}{T}, \frac{C_b}{T}, \frac{H}{T}, \frac{w}{T}, \frac{m_{piston} \Delta V}{\rho \cdot g^{1/2} T^{7/2}}, \left(\frac{g \cdot T^3 \rho^2}{\mu^2}\right), \pi_1 = \left(\frac{g^{1/2}}{T^{1/2} \cdot f}\right)\right) \quad (30)$$

In eqs 29 and 30, $\frac{t_m \cdot g^{1/2}}{T^{1/2}}$ is a dimensionless ratio that includes the mixing time t_m. $\frac{I}{\rho \cdot g^{1/2} T^{7/2}}$ and $\frac{m_{piston} \Delta V}{\rho \cdot g^{1/2} T^{7/2}}$ are two dimensionless numbers that quantify the impulse or the change in momentum induced by the beater, respectively. These two numbers are different ways to express the intensity of the collision at which the piston strikes the containers and could be theoretically or experimentally estimated. These values of the two dimensionless numbers are governed by the geometrical parameters of the crank/slider device (the crank radius R, the rod length L, and the distance from the rod pin to the piston pin l_1), by the distance separating the crankshaft center d_{sw} to the vertical tank wall, and by the angular crank frequency f. Indeed, depending on these physical quantities, the maximum penetration depth, the velocity at which the piston comes in contact with the soft container, and the length of time of the collision will be different, as previously explained.

$\pi_1 = \left(\frac{g^{1/2}}{T^{1/2} \cdot f}\right)$ is a dimensionless number that provides an internal measurement of the period of the clash. Consequently, the higher the angular crank frequency f is, the shorter the time between the two collisions will be, and the shorter the $\pi_1 = \left(\frac{g^{1/2}}{T^{1/2} \cdot f}\right)$ will be.

In eq 30, $Ga = \frac{g \cdot T^3 \rho^2}{\mu^2}$ is the SER Galilei number that provides an internal measure of how the viscosity of the fluid can influence the mixing process.

It was decided to make some rearrangements and to replace π_1 with ${\pi_1}^{-2}$ in order to make a modified Froude number, ${\pi_1}^{-2} = Fr$, appear. In this configuration, the Froude number, $Fr = \frac{f^2 \cdot T}{g}$, provides a measurement of beater frequency. Consequently, the higher the angular crank frequency is, the shorter the period of the collision is, the higher the Froude number is, and the higher the number of strikes delivered by the piston during a given period of time will be.

As a result, another π-space could be used to describe the SER mixing process

$$\frac{t_m \cdot g^{1/2}}{T^{1/2}} = F_6\left(\frac{h_1}{T}, \frac{h_2}{T}, \frac{r_2}{T}, \frac{E}{\rho \cdot Tg}, \frac{H_L}{T}, \frac{C_b}{T}, \frac{H}{T}, \frac{w}{T}, \frac{I}{\rho \cdot g^{1/2} T^{7/2}}, Fr, Ga\right) \quad (31)$$

$$\frac{t_m \cdot g^{1/2}}{T^{1/2}} = F_7\left(\frac{h_1}{T}, \frac{h_2}{T}, \frac{r_2}{T}, \frac{E}{\rho \cdot Tg}, \frac{H_L}{T}, \frac{C_b}{T}, \frac{H}{T}, \frac{w}{T}, \frac{m_{piston} \Delta V}{\rho \cdot g^{1/2} T^{7/2}}, Fr, Ga\right) \quad (32)$$

As explained by Delaplace et al. (2015) and White (2011), the choice of scaling variables and their recombinations is up to the users.[8,9] The choice will not affect the dimensional analysis but only the form of its presentation.

In the above section, the scaling of eqs 27 and 28 was performed by introducing (T, ρ, g) as repeated variables instead of using another basis that could be used for scaling such as (T, ρ, f). This choice was made so that the period $(1/f)$ of the beater strike appears only in one causal dimensionless number (in this case, $Fr = \frac{f^2 \cdot T}{g}$) and, consequently, isolate the influence of the beater frequency on the output (in our case, $\frac{t_m \cdot g^{1/2}}{T^{1/2}}$).

However, as in Delaplace et al. (2018), it is also possible to make some recombinations again from eqs 27 and 28 in order to give rise to different configurations (eqs 33−36) containing other dimensionless numbers such as $f \cdot t_m$ (instead of $\frac{t_m \cdot g^{1/2}}{T^{1/2}}$) or Reynolds numbers, $Re = \frac{\rho \cdot f \cdot T^2}{\mu}$ (instead of $Fr = \frac{f^2 \cdot T}{g}$), for which more physical significance could be intuitively captured and/or more commonly adopted in the mixing community.[7]

$f \cdot t_m$ is obtained by multiplying $\frac{t_m \cdot g^{1/2}}{T^{1/2}}$ by $(Fr)^{1/2}$, whereas the Reynolds number is derived from the recombination $(Ga \cdot Fr)^{1/2}$.

In this case, among the multiple possibilities, eqs 31 and 32 could become

$$\frac{t_m \cdot g^{1/2}}{T^{1/2}} = F_{12}\left(\frac{h_1}{T}, \frac{h_2}{T}, \frac{r_2}{T}, \frac{E}{\rho \cdot Tg}, \frac{H_L}{T}, \frac{C_b}{T}, \frac{H}{T}, \frac{w}{T}, \frac{I}{\rho \cdot g^{1/2} T^{7/2}}, Fr, Re\right) \quad (33)$$

$$\frac{t_m \cdot g^{1/2}}{T^{1/2}} = F_{13}\left(\frac{h_1}{T}, \frac{h_2}{T}, \frac{r_2}{T}, \frac{E}{\rho \cdot Tg}, \frac{H_L}{T}, \frac{C_b}{T}, \frac{H}{T}, \frac{w}{T}, \frac{m_{piston} \Delta V}{\rho \cdot g^{1/2} T^{7/2}}, Fr, Re\right) \quad (34)$$

https://dx.doi.org/10.1021/acs.iecr.9b06053
Ind. Eng. Chem. Res. 2020, 59, 6258−6268

$$f{\cdot}t_m = F_8\left(\frac{h_1}{T}, \frac{h_2}{T}, \frac{r_2}{T}, \frac{E}{\rho{\cdot}Tg}, \frac{H_L}{T}, \frac{C_b}{T}, \frac{H}{T}, \frac{w}{T}, \frac{I}{\rho{\cdot}g^{1/2}T^{7/2}}, Fr, Ga\right) \quad (35)$$

$$f{\cdot}t_m = F_9\left(\frac{h_1}{T}, \frac{h_2}{T}, \frac{r_2}{T}, \frac{E}{\rho{\cdot}Tg}, \frac{H_L}{T}, \frac{C_b}{T}, \frac{H}{T}, \frac{w}{T}, \frac{m_{piston}\Delta V}{\rho{\cdot}g^{1/2}T^{7/2}}, Fr, Ga\right) \quad (36)$$

$$f{\cdot}t_m = F_{10}\left(\frac{h_1}{T}, \frac{h_2}{T}, \frac{r_2}{T}, \frac{E}{\rho{\cdot}Tg}, \frac{H_L}{T}, \frac{C_b}{T}, \frac{H}{T}, \frac{w}{T}, \frac{I}{\rho{\cdot}g^{1/2}T^{7/2}}, Fr, Re\right) \quad (37)$$

$$f{\cdot}t_m = F_{11}\left(\frac{h_1}{T}, \frac{h_2}{T}, \frac{r_2}{T}, \frac{E}{\rho{\cdot}Tg}, \frac{H_L}{T}, \frac{C_b}{T}, \frac{H}{T}, \frac{w}{T}, \frac{m_{piston}\Delta V}{\rho{\cdot}g^{1/2}T^{7/2}}, Fr, Re\right) \quad (38)$$

When a given crank/slider device placed at a given bottom clearance is used to beat a given soft container filled with given viscous fluids at a constant liquid height, some geometrical ratios become fixed. Consequently, their effect on dimensionless mixing time could not be evaluated and the configurations should be reduced. In this case, eqs 31 and 38 become eqs 39 and 46.

$$f{\cdot}t_m = F_{14}\left(\frac{I}{\rho{\cdot}g^{1/2}T^{7/2}}, Fr, Ga\right) \quad (39)$$

$$f{\cdot}t_m = F_{15}\left(\frac{m_{piston}\Delta V}{\rho{\cdot}g^{1/2}T^{7/2}}, Fr, Ga\right) \quad (40)$$

$$f{\cdot}t_m = F_{16}\left(\frac{I}{\rho{\cdot}g^{1/2}T^{7/2}}, Fr, Re\right) \quad (41)$$

$$f{\cdot}t_m = F_{17}\left(\frac{m_{piston}\Delta V}{\rho{\cdot}g^{1/2}T^{7/2}}, Fr, \mathrm{Re}\right) \quad (42)$$

$$\frac{t_m{\cdot}g^{1/2}}{T^{1/2}} = F_{18}\left(\frac{I}{\rho{\cdot}g^{1/2}T^{7/2}}, Fr, Re\right) \quad (43)$$

$$\frac{t_m{\cdot}g^{1/2}}{T^{1/2}} = F_{19}\left(\frac{m_{piston}{\cdot}V}{\rho{\cdot}g^{1/2}T^{7/2}}, Fr, Re\right) \quad (44)$$

$$\frac{t_m{\cdot}g^{1/2}}{T^{1/2}} = F_{20}\left(\frac{I}{\rho{\cdot}g^{1/2}T^{7/2}}, Fr, Ga\right) \quad (45)$$

$$\frac{t_m{\cdot}g^{1/2}}{T^{1/2}} = F_{21}\left(\frac{m_{piston}{\cdot}V}{\rho{\cdot}g^{1/2}T^{7/2}}, Fr, Ga\right) \quad (46)$$

Note that when the physical properties of the agitated fluid (density and viscosity) are also maintained unchanged for a given mixing equipment, the Galilei number also becomes constant and the configuration is reduced as much as possible. Equations 39, 40, 45, and 46 become

$$f{\cdot}t_m = F_{22}\left(\frac{I}{\rho{\cdot}g^{1/2}T^{7/2}}, Fr\right) \quad (47)$$

$$f{\cdot}t_m = F_{23}\left(\frac{m_{piston}{\cdot}V}{\rho{\cdot}g^{1/2}T^{7/2}}, Fr\right) \quad (48)$$

$$\frac{t_m{\cdot}g^{1/2}}{T^{1/2}} = F_{24}\left(\frac{I}{\rho{\cdot}g^{1/2}T^{7/2}}, Fr\right) \quad (49)$$

$$\frac{t_m{\cdot}g^{1/2}}{T^{1/2}} = F_{25}\left(\frac{m_{piston}{\cdot}V}{\rho{\cdot}g^{1/2}T^{7/2}}, Fr\right) \quad (50)$$

The reduced π-spaces that appear in 39 will be used later to represent and to interpret the SER mixing time data measured for different operating conditions.

3.2. Homogenization Experiments and Computational Values of Dimensionless Numbers. SER mixing experiments were carried out using different Newtonian fluids placed in a soft elastic container with a fixed liquid height (see Materials and Methods). The measured mixing times are given in Table S1. For these trials, the bottom clearance position of the piston was maintained constant and equal to 0.025 m. Crank angular frequency and maximum penetration depth p (by adjusting the distance separating the crankshaft center to the vertical tank wall d_{sw}) were adapted accordingly.

In Table S1, mixing experiments are sorted into two groups: (i) the ones obtained at a fixed value of Galilei number (trials 1 to 15), involving a fluid with constant density (1263 kg m^{-3}) and Newtonian viscosity (1.25 Pa·s), and (ii) those obtained for varying values of Galilei number (trials 16 to 36), for which the fluid density and Newtonian viscosity range from 1190 to 1272 kg/m^3 and from 0.0285 to 1.187 Pa·s, respectively.

As a whole, 108 experiments (36 experiments × 3 times) were performed to determine the mixing times, but note that Table S1 only presents the average mixing time measured for each set of experimental conditions. The average standard deviation between repeated experiments for the 36 experiments was 10.4%.

Estimation of dimensional output parameters θ_c, t_c, $V(\theta = \theta_c)$, t_p, and I for the various imposed maximum penetration depths p and angular frequencies f (trials 1 to 36) are given in Table S2. The computed values of dimensionless numbers for the different mixing runs are given in Table S1.

Analysis of Table S2 shows us that the impulse dimensionless number and the change in momentum dimensionless number are equal. This result was expected because the impulse describes the change in the momentum of the SER, and the estimation of these two intermediate physical quantities can be derived from a similar analysis (namely, the kinetic motion of the piston). The only difference between the estimation of these two physical quantities is that the change in momentum required less assumptions (assuming no loss of forces during the transmission).

For the sake of brevity, only π-spaces involving dimensionless impulses (given in eqs 39, 41, 43, 45, 47, 49, and 51) were

https://dx.doi.org/10.1021/acs.iecr.9b06053
Ind. Eng. Chem. Res. 2020, 59, 6258−6268

considered to discuss the SER mixing time data in the following.

3.3. Influence of Frequency and Impulse on the Internal Measure of Mixing Time for Fixed Agitated Media. The evolution of the dimensionless SER mixing time based on the reduced configuration presented in eq 49 is represented in Figure 4. The value of the Galilei number for this set of experiments was fixed (trials 1 to 15) and is equal to 1252. Because the Galilei number is fixed, the effect of the viscosity of the fluid in the container on mixing time are assumed to be constant and could not be interpreted (see eq 49). Each symbol represents one mixing time experiment. For each symbol, the value of the impulse dimensionless number, $\frac{I}{\rho \cdot g^{1/2} T^{7/2}}$, for which the mixing experiment was conducted is given in the legend. It should be recalled that each couple (p,f) (representing the maximum penetration depth and beater frequency), which are the commands of the mixing process, leads to one impulse value. The three different colors used for the symbols are visual guides for the three imposed maximum penetration depths. Red, orange, and green are for the maximum penetration depths of 0.015, 0.02, and 0.025 m, respectively.

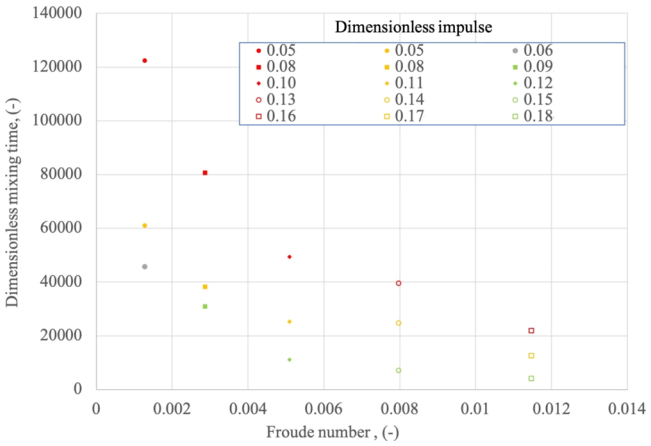

Figure 4. Evolution of dimensionless mixing time for the SER $\frac{t_m \cdot g^{1/2}}{T^{1/2}}$ as a function of the modified Froude number $Fr = \left(\frac{f^2 \cdot T}{g}\right)$.

Figure 4 plots the evolution of $\left(\frac{t_m \cdot g^{1/2}}{T^{1/2}}\right)$ versus Fr. As previously explained, the Froude number, $Fr = \left(\frac{f^2 \cdot T}{g}\right)$, is an internal measure of the beater frequency, and $\left(\frac{t_m \cdot g^{1/2}}{T^{1/2}}\right)$ represents an internal measurement of the dimensionless mixing time.

Figure 4 reveals that both the beater frequency and the impulse values strongly affect the dimensionless mixing time number.

At a given Froude number (beater frequency), a drastic decrease of dimensionless mixing time is observed for a small increase in the dimensionless impulse number. It can be concluded that for a fixed beater frequency, the greater the impulse is, the faster the desired degree of homogeneity will be. It can also be observed that the decrease in mixing time with the increase in impulse is more pronounced when the beater frequency is low. For the range of Froude numbers investigated, it is clear that the beater frequency has less impact on dimensionless mixing time than an increase in impulse. These data describing the influence of impulse and frequency of collision on mixing time data are consistent with the expected physical trends.

Figure 5 is another representation of the evolution of the dimensionless SER mixing time, this time is based on the reduced configuration of eq 47. In this figure, the number of strikes needed to reach complete homogenization, $f \cdot t_m$, is plotted on the ordinate axis.

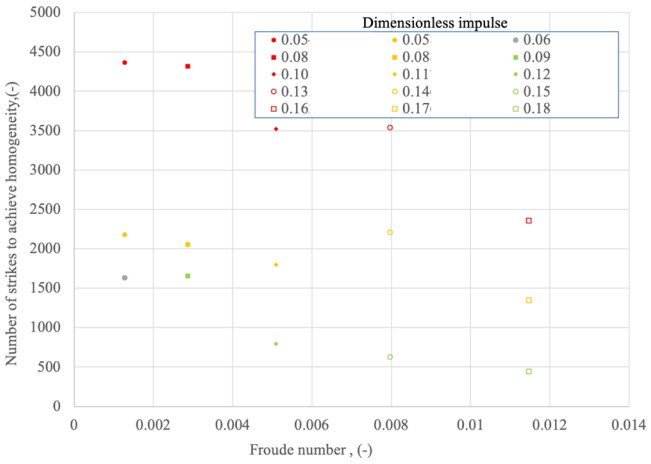

Figure 5. Number of strikes of the piston required to achieve the desired level of homogeneity, $f \cdot t_m$, as a function of the modified Froude number, $Fr = \left(\frac{f^2 \cdot T}{g}\right)$.

Figure 5 clearly shows that the number of strikes needed to reach complete homogenization in the SER is markedly influenced by the Froude number (beater frequency) and the impulse dimensionless values. For the range of Froude numbers and impulse dimensionless values considered, it appears that the impulse dimensionless number and the Froude number should be maximal in order to minimize the number of strikes.

To better quantify the effect of the impulse and frequency on the mixing process in the SER, it was decided in the next section to determine whether or not a predictive empirical correlation could be established. The number of strikes for achieving homogeneity was taken as the target variable.

3.4. Correlation for Predicting the Number of Strikes Needed for Reaching Homogeneity. The mixing process (and, consequently, the number of strikes needed for reaching a given homogeneity level) is assumed to be impacted by the viscosity of liquids in the container. As a consequence, an internal measurement appears in the dimensionless configuration to take the influence of viscosity (either the Galilei number in eq 39 or the Reynolds number in eq 41) into account. However, we can observe that if mixing experiments are performed in a given soft reactor with a fixed fluid, the Galilei number becomes constant. As previously mentioned, this situation is interesting because the number of strikes becomes only a function of the impulse number and the Froude number, facilitating the determination of a mathematical equation for the process relationship. Therefore, in a first step, only experimental data obtained at a fixed Galilei number (Ga = 1252) were retained (trials 1 to 16) to identify the process relationship:

https://dx.doi.org/10.1021/acs.iecr.9b06053
Ind. Eng. Chem. Res. 2020, 59, 6258−6268

The following simple relationship could be proposed

$$f \cdot t_m = A'\left(\frac{I}{\rho \cdot g^{1/2} T^{7/2}}\right) + B' \tag{51}$$

where A' and B' are two power law functions of the Froude number

$$A' = -6766.9\, Fr^{-1.114} \tag{52}$$

$$B' = 11{,}077\, Fr^{-0.632} \tag{53}$$

Equation 51 is validated for

$$1.2710^{-3} < Fr < 1.1510^{-2};$$

$$6.1410^{-2} < \left(\frac{I}{\rho \cdot g^{1/2} T^{7/2}}\right) < 1.6210^{-1}; \qquad Ga = 1252$$

For a fixed Galilei number (Ga = 1252), the agreement between experimental and predicted data is good, as can be seen in Figure 6.

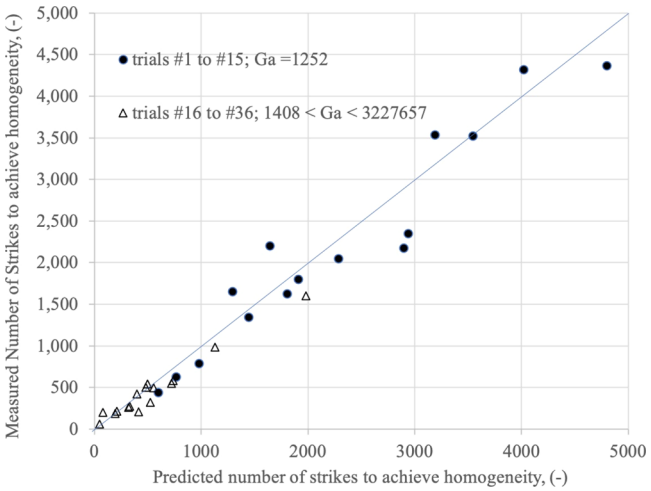

Figure 6. Comparison between experimental and predicted values of the number of strikes needed for reaching homogeneity in the SER based on 51.

For higher values of the Galilei number (ranging from 1252 to 3,227,657 from trials 17 to 32), it can be observed (Figure 6) that predictive correlation progressively deviates from experimental values, leading to considerable scatters up to Galilei number values greater than 2200.

In order to go further and to find a predictive correlation that could be validated for the different fluids within the container of the SER, fitting with the help of a symbolic regression program (Eureqa) was attempted. All the experimental data were considered, taking the number of strikes as outcome variables. π-spaces appearing in eq 41 were chosen to correlate the results because Reynolds and Froude numbers are more commonly adopted in the mixing community to describe viscosity and liquid-free surface deformation influences on the mixing process.

As was previously mentioned, a symbolic regression program could be very helpful to identify process relationships.[10,11] Because a sigmoid shape is expected for the evolution of the number of strikes as a function of Reynolds number for a given penetration depth ratio,[7] the corresponding mathematical model was looking forward in priority.

Thus, an empirical correlation describing the evolution of the number of strikes needed for reaching homogenization as a function of the Reynolds number and impulse number can be obtained. The mathematical equation of this correlation is given below

$$\Theta_m = f \cdot t_m = \frac{\left(D\left(\frac{I}{\rho \cdot g^{1/2} T^{7/2}}\right)^{-11.697} + E + 5.577\right)}{(1 + 0.569 \cdot \mathrm{Re}^{-0.193})^{-12.106}} - 5.577 \tag{54}$$

$$D = +20{,}642.9\, Fr^{6.172} \tag{55}$$

$$E = -135.4\, Fr^{0.699} \tag{56}$$

Equation 54 is validated for

$$1.3 < Re < 193; \qquad 1.27 \times 10^{-3} < Fr < 4.59 \times 10^{-2}$$

$$; \qquad 6.14\ 10^{-2} < \left(\frac{I}{\rho \cdot g^{1/2} T^{7/2}}\right) < 3.6610^{-1}$$

Figure 7 shows that a good agreement is observed for the whole set of data (the correlation coefficient is equal to 0.977).

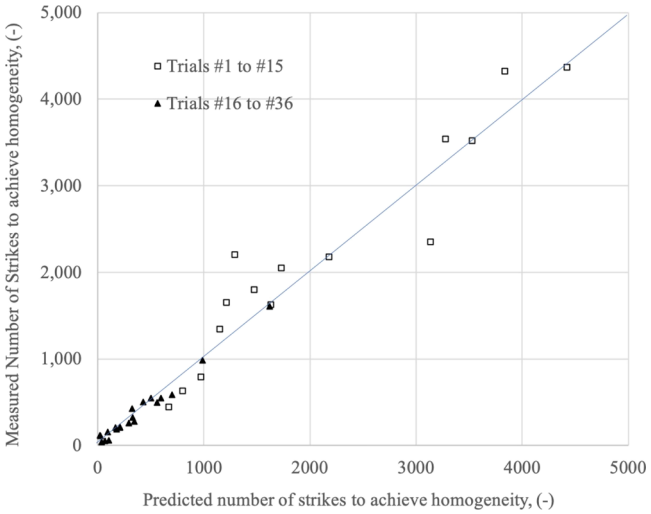

Figure 7. Predicted and experimental values for the number of strikes needed for reaching homogeneity. Experimental data are those given in Table S1.

The standard deviation between experimental data and predicted values is equal to 21%. One difficulty here is to predict the number of strikes required for mixing processes that take place in transition and turbulent regimes as the decrease in the number of strikes is very significant beyond the laminar regime and little experimental data are available to precisely identify the shape of the curve in these cases.

4. CONCLUSIONS

In this study, mechanistic models linking the inlet parameters of the crank/slider device responsible for the tank wall vibrations to the mixing times were established for the SER. The mechanistic models are based on dimensional analysis and

https://dx.doi.org/10.1021/acs.iecr.9b06053
Ind. Eng. Chem. Res. 2020, 59, 6258−6268

involve intermediate parameters with strong physical significance such as impulse and change in momentum. These intermediate quantities are derived from theoretical considerations. They are introduced in the relevant list to take the intensity of mechanical solicitation induced by the beater into account. Several π-spaces were established to represent the SER mixing process, involving these intermediate quantities.

The experimental results showed that the number of strikes needed to reach a given degree of homogeneity is influenced by the Reynolds number, the impulse dimensionless number, and the frequency of strikes. Finally, predictive correlations were obtained that covered various flow regimes, with a standard deviation within 20%.

■ ASSOCIATED CONTENT

Supporting Information

The Supporting Information is available free of charge at https://pubs.acs.org/doi/10.1021/acs.iecr.9b06053.

Mixing time obtained when homogenizing a given fluid (μ, ρ) in the SER and computed value of dimensionless numbers for the different trials (1 to 36) and estimation of output parameters θ_c, t_c, $V(\theta = \theta_c)$, t_p, and I for the cases with different maximum penetration depths p and angular frequencies f (trials 1 to 36) (PDF)

■ AUTHOR INFORMATION

Corresponding Authors

Guillaume Delaplace − *International Associated Laboratory-FOODPRINT (INRAE and Institut Agro (France)-Soochow University (China)), Soochow University, Suzhou, Jiangsu 215123, China; UMET - Unité Matériaux et Transformations, UMR 8207 (Univ. Lille, CNRS, INRAE, Centrale Lille), F-59000 Lille, France*; Email: Guillaume.Delaplace@inrae.fr

Jie Xiao − *International Associated Laboratory-FOODPRINT (INRAE and Institut Agro (France)-Soochow University (China)) and School of Chemical and Environmental Engineering, College of Chemistry, Chemical Engineering and Materials Science, Soochow University, Suzhou, Jiangsu 215123, China;* orcid.org/0000-0001-7842-7862; Email: jie.xiao@suda.edu.cn

Authors

Minghui Liu − *School of Chemical and Environmental Engineering, College of Chemistry, Chemical Engineering and Materials Science, Soochow University, Suzhou, Jiangsu 215123, China*

Romain Jeantet − *International Associated Laboratory-FOODPRINT (INRAE and Institut Agro (France)-Soochow University (China)), Soochow University, Suzhou, Jiangsu 215123, China; STLO, INRAE, Institut Agro, 35042 Rennes, France*

Xiao Dong Chen − *International Associated Laboratory-FOODPRINT (INRAE and Institut Agro (France)-Soochow University (China)) and School of Chemical and Environmental Engineering, College of Chemistry, Chemical Engineering and Materials Science, Soochow University, Suzhou, Jiangsu 215123, China*

Complete contact information is available at: https://pubs.acs.org/10.1021/acs.iecr.9b06053

Notes

The authors declare no competing financial interest.

■ ACKNOWLEDGMENTS

The authors deeply thank the National Key R&D Program of China (International S&T Cooperation Program, ISTCP, 2016YFE0101200), the National Natural Science Foundation of China (21676172 and 21978184), the Natural Science Foundation of Jiangsu Province (BK20170062), and the "Priority Academic Program Development (PAPD) of Jiangsu Higher Education Institutions" for their financial support. J.X. also acknowledges the "Jiangsu Innovation and Entrepreneurship (ShuangChuang) Program" and the "Jiangsu Specially-Appointed Professors Program".

■ NOTATION

C_b	bottom clearance of the SER beater, m
E	Young's modulus of the elastic material composing the SER wall, Pa
f	crank angular frequency and strike frequency, s^{-1}
Fr	SER Froude number (eq 31)
Ga	SER Galilei number (eq 3)
H	beater height, m
H_L	liquid height in the tank, m
h_1	SER tank height, m
h_2	SER base height, m
$\frac{I}{\rho \cdot g^{1/2} T^{7/2}}$	SER impulse number (eq 29)
p	maximum penetration depth, m
Re	SER Reynolds number (eq 2)
R	crank radius, m
L	rod length, m
l_1	distance from the rod pin to the piston pin, m
t	time, s
t_m	SER mixing time, s
T	inner diameter of the vessel, m
$\frac{m_{piston}\Delta V}{\rho \cdot g^{1/2} T^{7/2}}$	dimensionless number quantifying the change in momentum

■ GREEK LETTERS

μ	Newtonian viscosity, Pa·s
ρ	liquid density, kg m^{-3}

■ REFERENCES

(1) Chen, X. D. Scoping Biology-Inspired Chemical Engineering. *Chin. J. Chem. Eng.* **2016**, *24*, 1−8.

(2) Chen, X. D.; Liu, M. Material preparation and procedures for making a soft elastic reactor and the methods for mixing in this reactor. CN 104841299 A, 2015.

(3) Liu, M.; Xiao, J.; Chen, X. D. A Soft-Elastic Reactor Inspired by the Animal Upper Digestion Tract. *Chem. Eng. Technol.* **2018**, *41*, 1051−1056.

(4) Liu, M. H.; Zou, C.; Xiao, J.; Chen, X. D. Soft-Elastic Bionic Reactor. *CIESC J.* **2018**, *69*, 414−422.

(5) Xiao, J.; Zou, C.; Liu, M.; Zhang, G.; Delaplace, G.; Jeantet, R.; Chen, X. D. Mixing in A Soft-Elastic Reactor (SER) Characterized Using An RGB Based Image Analysis Method. *Chem. Eng. Sci.* **2018**, *181*, 272−285.

(6) Zhang, G.; Liu, M.; Zou, C.; Xiao, J.; Chen, X. D. Enhancement of Liquid Mixing in A Soft-Elastic Reactor based on Bionics with An Elastic Rod. *Chem. Ind. Eng. Prog.* **2019**, *38*, 826−833.

(7) Delaplace, G.; Gu, Y.; Liu, M.; Jeantet, R.; Xiao, J.; Chen, X. D. Homogenization of Liquids Inside A New Soft Elastic Reactor: Revealing Mixing Behavior Through Dimensional Analysis. *Chem. Eng. Sci.* **2018**, *192*, 1071−1080.

(8) Delaplace, G.; Loubiere, K.; Ducept, F.; Jeantet, R. *Dimensional Analysis of Food Processes*; ISTE Press—Elsevier, 2015.

(9) White, F. M. *Fluid Mechanics*; McGraw-Hill Series in Mechanical Engineering; McGraw-Hill Publishing Co., 2011.
(10) Stoutemyer, D. R. Dimensional Analysis, Using Computer Symbolic Mathematics. *J. Comput. Phys.* **1977**, *24*, 141−149.
(11) Stoutemyer, D. R. Can the Eureqa Symbolic Regression Program, Computer Algebra, and Numerical Analysis Help Each Other? *Not. AMS* **2013**, *60*, 713−724.

https://dx.doi.org/10.1021/acs.iecr.9b06053
Ind. Eng. Chem. Res. 2020, 59, 6258−6268